JSAEM Studies in Applied Electromagnetics, 4

ELECTROMAGNETIC PHENOMENA APPLIED TO TECHNOLOGY

Proceedings of
The Fourth Japanese and Polish Joint Seminar
on Electromagnetic Phenomena Applied to Technology
June 5 - 7, 1995, Oita, Japan

Supplement to Volume 4 of the Journal of the
Japan Society of Applied Electromagnetics
and Mechanics

Editors

Masato Enokizono

Faculty of Engineering
Oita University
Oita, Japan

Takashi Todaka

Faculty of Engineering
Oita University
Oita, Japan

Electromagnetic Phenomena Applied to Technology
M. Enokizono and T. Todaka (eds.)

THE INFLUENCE OF MESH DENSITY IN 3-D EDDY-CURRENT ANALYSIS USING FIRST ORDER EDGE-BASED FINITE ELEMENTS OF MIXED TYPE

Vlatko Čingoski and Hideo Yamashita

Electric Machinery Laboratory,
Faculty of Engineering,
Hiroshima University,
Kagamiyama 1-4-1, Higashihiroshima, 739 Japan

ABSTRACT

In this paper, the problem of defining the optimal mesh density for accurate computation of 3-D eddy-current distribution using first-order edge-based finite elements of mixed type is presented. The accuracy of eddy-current distribution is investigated using various finite element mesh densities both inside and outside the penetration area of eddy-current flow. All three components of eddy-current vectors were monitored by developing a 3-D test model. The 3-D test model and the obtained results for eddy-current distribution and eddy-current losses are presented in detail. Construction of an optimal mesh density division is discussed along with conclusions and points for future research, especially for the development of h- and r-adaptive mesh procedures.

INTRODUCTION

Eddy-current distribution is important in analysis and design of various electromagnetic devices such as motors and generators, induction heating devices, levitation and continuous casting devices. Therefore, in the computation of eddy-current distribution, speed, simplicity and accuracy are of utmost importance. A widely employed method for analysis of eddy-current phenomena in electromagnetic devices is the finite element method. Recently, vector finite elements were proposed for 3-D magnetic field analysis [1]. Mainly due to their computational advantages, these vector finite elements, 'edge-based' if they are associated with the edges of a finite element mesh, or 'facet-based' if they are associated with the facets of a finite element mesh, have become frequently employed for solution of various 3-D magnetic or eddy-current problems [2]. Therefore, the finite element method with edge-based finite elements of mixed type [2] allows fast and accurate analysis with less computational efforts and memory requirements [3], [4]. Due to some peculiarities of the edge-based finite elements, however, the problem of the construction of an optimal mesh division, resulting in accurate eddy-current distribution and eddy-current losses, still exists. This problem is even more acute for high-frequency problems with very small penetration depths of the eddy-current distribution.

In this paper, results obtained during investigation of the influence of mesh density on the results obtained for 3-D eddy-current finite element analysis using the first-order edge-based finite elements of mixed type are presented. A 3-D test model was developed to monitor all three components of eddy-current density vectors and their changes due to various mesh densities inside and outside the penetration depths of the eddy-current flow area. For mesh divisions with various density, the

spatial eddy-current intensity and vector distributions were obtained. The eddy-current distributions along a few typical lines inside the analyzed model were derived and compared for the case of various mesh divisions. Finally, conclusions and points for future research, especially for the development of h- and r-adaptive finite element meshes, are given.

THE ANALYZED MODEL

The analysis of 3-D eddy-current distribution due to the construction of division meshes with various densities is performed using the 3-D test model presented in Fig. 1. The model consists of an air-cored coil positioned over a hollow aluminum plate. The electrical parameters of the analyzed model are: source current $I_0 = 1000\ [AT]$ and frequency $f = 100\ [Hz]$. The conductivity of the aluminum plate is $\sigma_{Al} = 3.817 \cdot 10^7\ [m/\Omega \cdot m^2]$ which results in penetration depths of the eddy-current flow inside the aluminum plate of $\delta = \sqrt{\frac{2}{2\pi f \sigma_{Al} \mu_0}} = 8.146\ [mm]$.

Two typical mesh divisions, course mesh - Model 2 and dense mesh - Model 5, are presented in Fig. 2. In order to achieve different mesh divisions inside and outside the penetration area, the area of consideration was divided into three separate domains A, B and C (see Fig. 3), for which various mesh divisions were developed. Typical mesh divisions to which the eddy-current distributions were compared are presented in Table I. We were able to develop rough and dense division meshes for the penetration area and the non-penetration area separately, and we also created combinations, e.g., dense mesh for the penetration area and rough mesh for the non-penetration area, and vice versa.

Table I. *Analyzed models with domain division meshes*

	Model 1	Model 2	Model 3	Model 4	Model 5
Domain A - $20 \times 100\ [mm \times mm]$	2×10	4×10	8×13	8×13	8×13
Domain B - $10 \times 50\ [mm \times mm]$	1×5	2×5	4×7	4×7	4×7
Domain C - $20 \times 150\ [mm \times mm]$	1×15	2×15	1×20	4×20	6×20

RESULTS AND DISCUSSION

The results of the analysis can be classified into two major groups: 3-D distributions and data for eddy-current losses. Regarding 3-D distributions, we obtained the spatial distribution of an eddy-current density vector inside the aluminum plate, in other words, its intensity and vector distributions. In order to compare the results numerically, the amplitudes of the eddy-current vector were calculated along three typical lines inside the analyzed model and presented in Fig 4:

- Line 1, going along x direction from 0 to 150 $[mm]$ and for constant $y = 50\ [mm]$ and $z = 40\ [mm]$ coordinates,
- Line 2, going along x direction from 0 to 150 $[mm]$ and for constant $y = 50\ [mm]$ and $z = 30\ [mm]$ coordinates, and

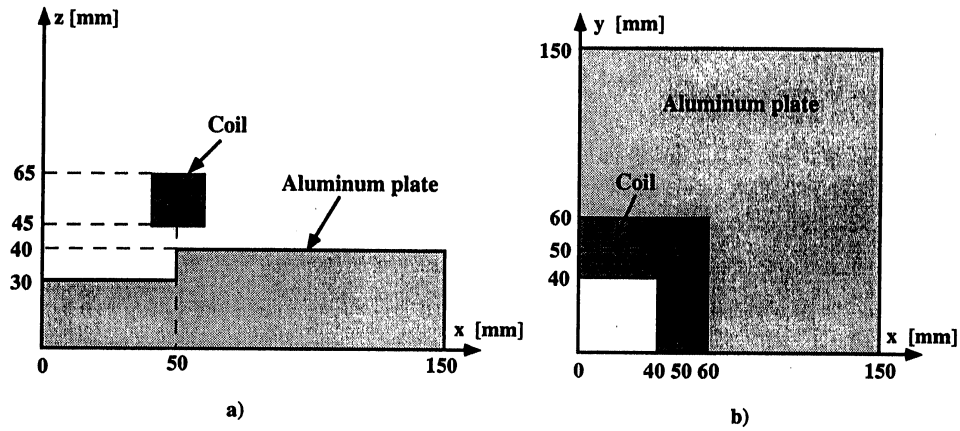

Fig. 1. Analyzed model. a) front view, b) top view

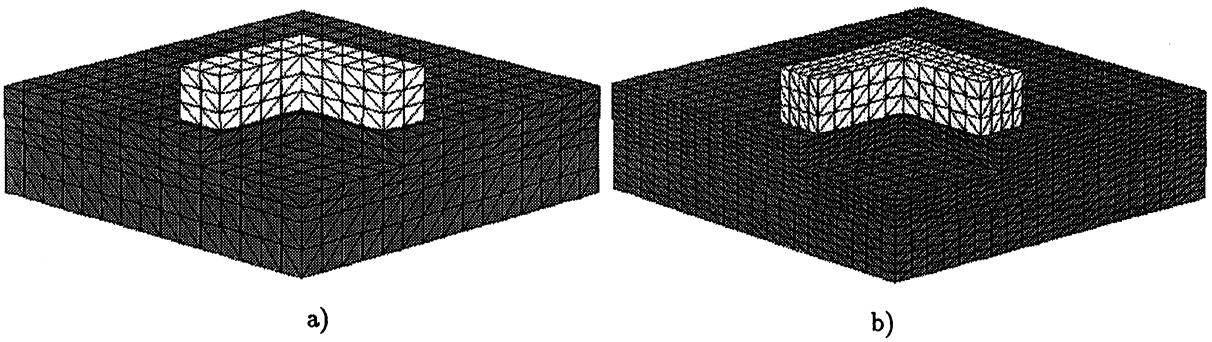

Fig. 2 Mesh divisions: a) course mesh b) dense mesh

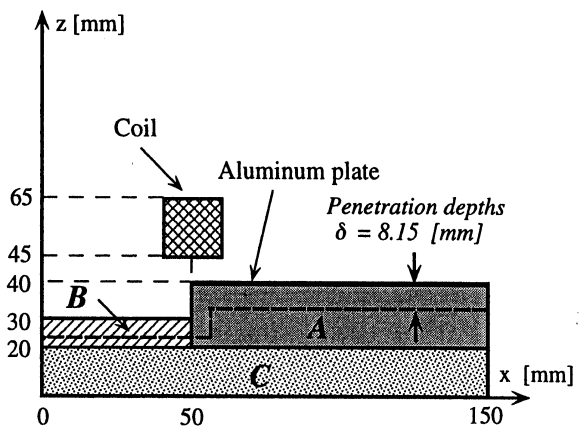

Fig. 3. Area of interest with domains A, B and C.

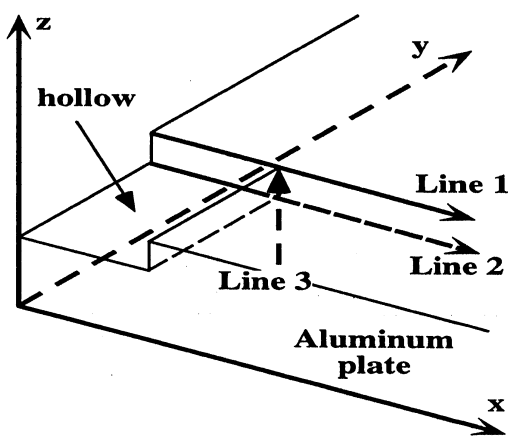

Fig. 4. Three typical lines inside analyzed model.

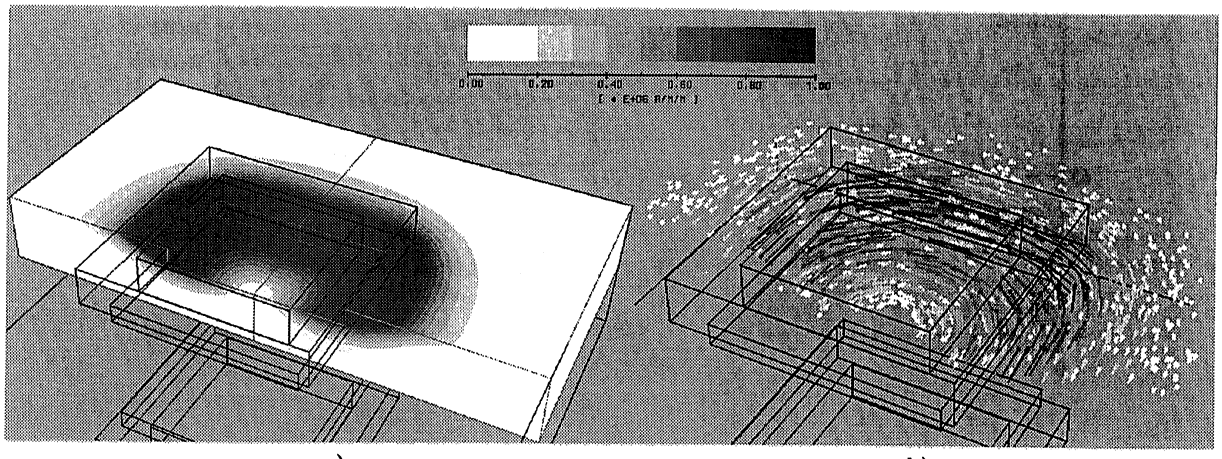

a) b)

Fig. 5 Eddy-current density vector $\mathbf{J}_e$. a) 3D intensity distribution, b) 3D vector distribution

- Line 3, going along z direction from 0 to 40 $[mm]$ and for constant $x = 50$ $[mm]$ and $y = 50$ $[mm]$ coordinates.

The 3-D intensity and vector distributions of eddy-current density vector $\mathbf{J}_e$ are presented in Figs. 5 *a* and *b*, respectively. The influence of the mesh density inside and outside the penetration area was investigated separately.

Inside Penetration Area

Models 1, 2 and 5 were monitored in order to compare the eddy-current distribution for different mesh densities inside the penetration area. Model 5 was established as a standard, while Models 1 and 2 were treated as rough and medium dense division meshes, respectively. The obtained eddy-current distributions along the aforementioned typical lines 1, 2 and 3 for each model are presented in Figs. 6 *a*, *b* and *c* respectively. From Fig. 6, it is apparent that as the mesh density increases, the accuracy of the results improves. This can be further verified using relative error diagrams which are presented in Figs. 7 *a*, *b* and *c*. The relative errors are computed by the following equation:

$$\textit{Relative error } \varepsilon_i = \frac{Var^{Model\ 5} - Var^{Model\ k}}{Var^{Model\ 5}} \cdot 100\ [\%]\,, \tag{1}$$

using results of the Model 5 (see Table I) as a standard values. In Eq. 1, Var can be any arbitrary variable such as magnetic flux intensity, eddy-current intensity or eddy-current losses, while k stands for 1, 2, 3 or 4.

The largest discrepancy in the results can be observed near the plane of symmetry (boundary plane) and at the corner of the hollow (Fig. 4). This could be attributed to the type of the edge-based finite element employed in the analysis. A first order 'edge-based' finite element of mixed type with only six unknowns per tetrahedron, employed in this analysis, provides a large computational savings in time and memory; it usually results, however, in poor convergence rate and has an accuracy of order $O(h)$, where h denotes the largest dimension of the tetrahedron [2]. Further

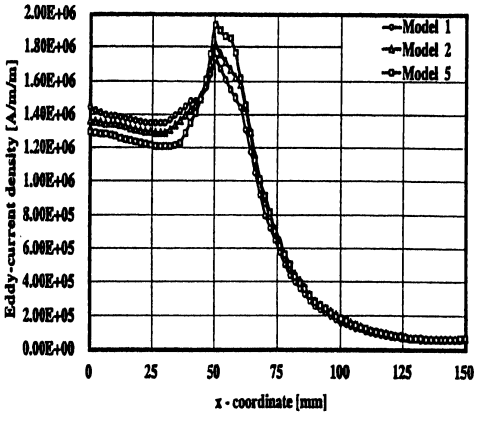

a) Along Line 1

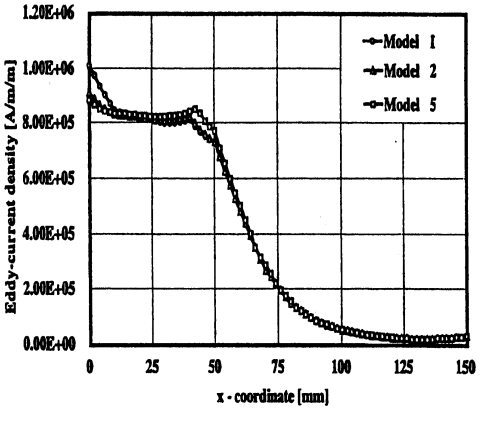

b) Along Line 2

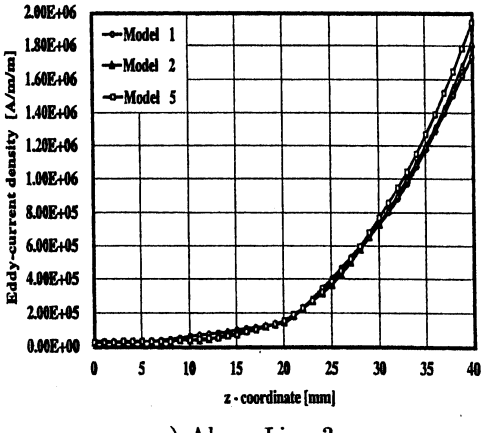

c) Along Line 3

Fig. 6 Eddy-current distribution for different mesh densities inside penetration depth area.

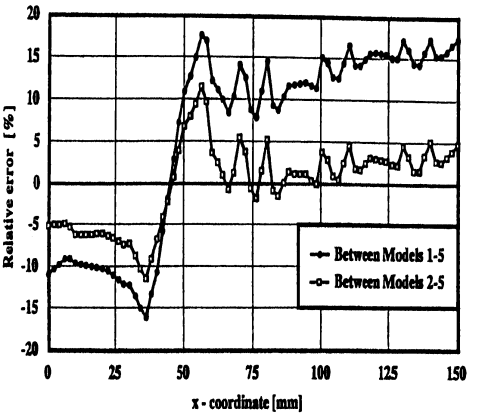

a) Along Line 1

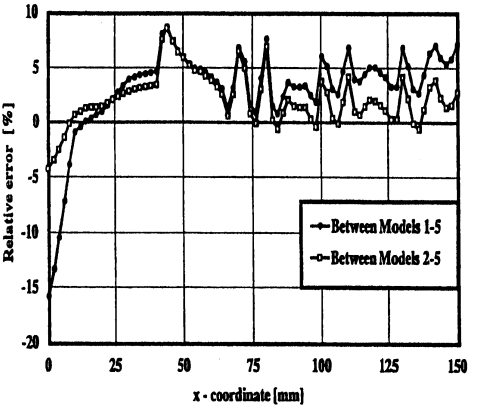

b) Along Line 2

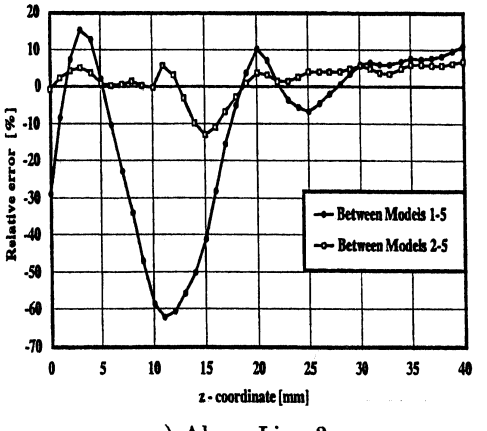

c) Along Line 3

Fig. 7 Relative error distribution for different mesh densities inside penetration depth area.

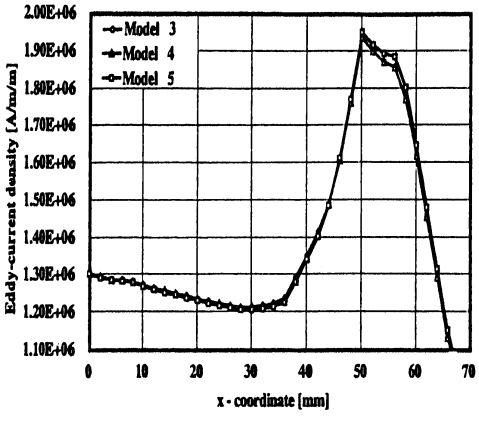

a) Along Line 1

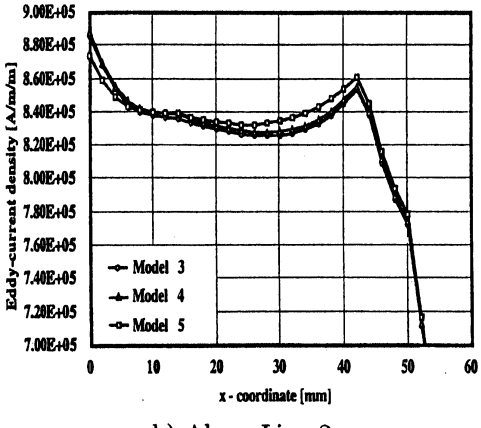

b) Along Line 2

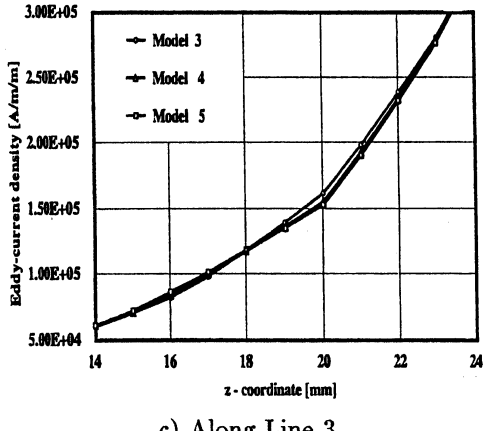

c) Along Line 3

Fig. 8 Eddy-current distribution for different mesh densities outside penetration depth area.

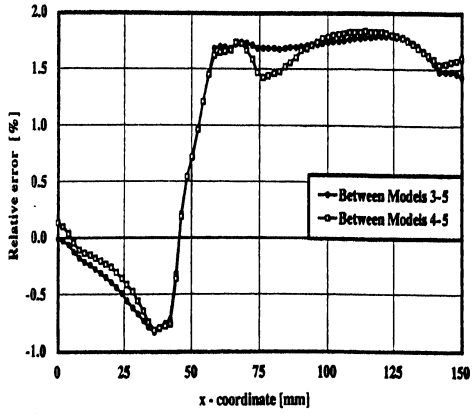

a) Along Line 1

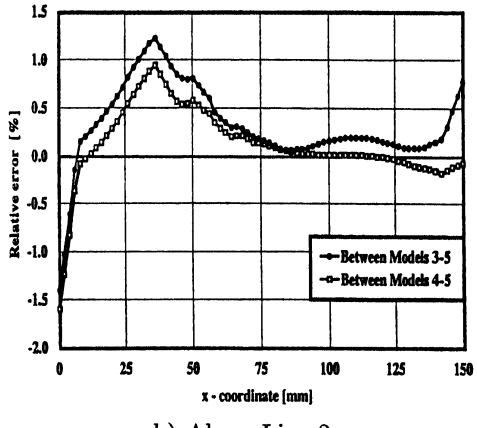

b) Along Line 2

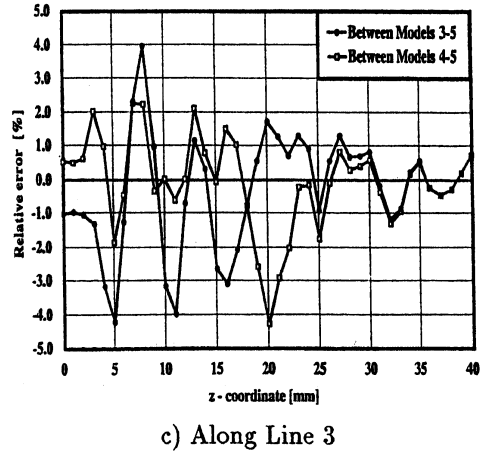

c) Along Line 3

Fig. 9 Relative error distribution for different mesh densities outside penetration depth area.

investigation, using the so called *Consistently linear edge finite elements* [2] having twelve unknown variables for each tetrahedron (two per edge) and accuracy of order $O(h^2)$ could be plausible.

Outside Penetration Area

The development of a very rough mesh outside the penetration area of eddy-current flow is common. In our research we wanted to examine how this mesh roughness influences the accuracy of the eddy-current results. Therefore, to investigate the influence of mesh density outside the penetration area, three different division meshes were developed – Models 3, 4 and 5. The eddy-current distributions were obtained along the aforementioned typical lines 1, 2 and 3 and are presented in Figs. 8 *a*, *b* and *c*. Figures 9 *a*, *b* and *c* show the relative error of eddy-current distribution along each of the typical lines 1, 2 and 3. In this case, the obtained results were very close to each other, confirming that the influence of mesh density outside the penetration area is insignificant. However, too rough a mesh is not advisable in order to keep the desired accuracy of the obtained eddy-current distribution.

Eddy-current Losses

Besides the aforementioned 3-D eddy-current distributions for the entire analysis domain or along few typical lines, we also analyzed some other, rather numerical data, such as the maximum and minimum intensity values of magnetic flux density vector, eddy-current density vector and eddy-current losses. The results obtained for maximum intensity values of magnetic flux density vector **B** and eddy-current density vector $\mathbf{J}_e$, eddy-current losses and other relevant data for each of the analyzed models are presented in Table II. The relative errors computed using Eq. 1 for Model 5 as a standard are also given in Table II.

Table II. *Selected input and output data*

	Model 1	Model 2	Model 3	Model 4	Model 5
Points	5072	5696	10093	11376	12392
Elements	26208	29638	54386	61718	67506
Edges	32494	36641	66281	75000	81894
B_{max} [*Gauss*]	166.87(−14.32%)	168.03(−13.72%)	194.95(0.364%)	194.76(0.004%)	194.76
J_{emax} $[A/m^2] \cdot 10^7$	0.2964(−1.496%)	0.2955(−1.790%)	0.3016(0.212%)	0.3009(0.003%)	0.3008
Eddy-current losses [*W*]	6.829(11.575%)	6.318(3.227%)	6.117(−0.065%)	6.119(−0.024%)	6.121

CONCLUSIONS

From the results obtained during the analysis, a conclusion can be drawn that the 3-D edge-based finite element of mixed type deals very easily and accurately with eddy-current problems. Even relatively rough mesh of the same order with the penetration depths of eddy-current flow can be appropriate for initial analysis, although for very accurate analysis more dense division mesh is advisable. In order to develop an optimal mesh and establish conditions that have to be satisfied

during the adaptive re-meshing process using h- and r-adaptive procedures, the following must be taken into consideration:

- Mesh with at least two finite elements inside the penetration depths of eddy-currents can always be accepted as a sufficiently accurate approximation to the real one.
- In order to develop an optimal mesh from CPU time and memory point of view, and at the same time, obtain an accurate solution of the problem, the mesh has to be dense enough only inside the penetration area of eddy-current flow. At the same time, the generated finite element mesh outside the penetration area should not be too rough. A kind of gradually dense mesh, going from non-penetration area toward penetration area, with finite elements, finite elements with edges of approximately same lengths is strongly advisable.

References

[1] M. L. Barton and Z. J. Cendes: "New vector finite elements for three-dimensional magnetic field computation", *Journal of Applied Physics*, Vol. 61, No. 8, 15 April 1987, pp.3919-3921.

[2] G. Mur: "Edge Elements, their Advantages and their Disadvantages", *IEEE Transactions on Magnetics*, Vol. 30, No. 5, September 1994, pp.3552-3557.

[3] A. Kameari: "Calculation of transient 3D eddy current using edge-elements", *IEEE Transactions on Magnetics*, Vol. 26, No. 2, March 1990, pp.466-469.

[4] T. Nakata, N. Takahashi, K. Fujiwara, T. Imai and K. Muramatsu: "Comparison of various methods of analysis and finite elements in 3-D magnetic field analysis", *IEEE Transactions on Magnetics*, Vol. 27, No. 5, September 1991, pp.4073-4076.